JOURNAL OF Materials CHEMISTRY

Evolution of the cluster glass system $La_{0.5}Sr_{0.5}CoO_3$

Kumar P. S. Anil,[a] Santhosh P. N. Nair,[b] Joy P. Alias*[b] and Sadgopal K. Date[b]

[a] *Centre for Advanced Studies in Materials Science and Solid State Physics, Department of Physics, University of Pune, Pune 411007, India*
[b] *Physical and Materials Chemistry Division, National Chemical Laboratory, Pune 411008, India. E-mail: joy@dalton.ncl.res.in*

Received 21st April 1998, Accepted 30th June 1998

The electrical and magnetic properties of the $x=0.5$ composition in the perovskite system $La_{1-x}Sr_xCoO_3$, annealed in air at different temperatures, have been investigated. Results from powder XRD, ac magnetic susceptibility, high field and low field (FC and ZFC) dc magnetization, electrical resistivity and EDAX measurements revealed that differences in the properties between the samples annealed at different temperatures (1000–1300 °C) arise due to compositional inhomogeneity. A true compositionally homogeneous compound is formed when annealed in a narrow temperature region close to *ca.* 1150 °C. A pronounced resistivity anomaly at the Curie temperature with a maximum temperature coefficient of resistance and a well defined magnetic transition are observed for the samples annealed at 1150 °C. The results can explain most of the unusual and widely differing results reported in the literature on the electronic and magnetic properties of different compositions in the $La_{1-x}Sr_xCoO_3$ system which are synthesized and processed at different temperatures.

Introduction

The perovskite systems based on $La_{1-x}A_xMO_3$ compositions (where A = Ca, Sr, Ba, *etc.* and M = Mn, Co) have been studied extensively for the past four decades because of their interesting electrical and magnetic properties.[1–11] In the recent past, there is a renewed interest in the study of these systems because of the colossal magnetoresistance (CMR) shown by the manganates (M = Mn).[7] The cobaltates, on the other hand (M = Co) exhibit low magnetoresistance (MR).[8–11] CMR effect in the manganates is coupled with the Jahn–Teller distortion of the MnO_6 octahedra containing Mn^{3+} (d^4 ion) and it has been reported that there is a distortion of the structure of the manganates at the Curie temperature where maximum MR effect is observed.[12,13] Among the corresponding cobaltates, the system $La_{1-x}Sr_xCoO_3$ has been extensively studied in connection with the onset of ferromagnetism and insulator–metal (I–M) transition on Sr doping and the high metallic conductivity of Sr-rich compositions. The compound $La_{0.5}Sr_{0.5}CoO_3$ shows close resemblance with cuprate superconductors, though the system does not show any signs of superconductivity down to lowest temperatures.[14]

In pure stoichiometric $LaCoO_3$, cobalt is present in the low-spin Co^{III} state at low temperatures and it exhibits a low-spin ($t_{2g}{}^6e_g{}^0$)–high-spin ($t_{2g}{}^4e_g{}^2$) state equilibrium in the temperature range 400–600 K.[15–18] The substitutional effects of Sr^{2+} in $La_{1-x}Sr_xCoO_3$ ($0 \leqslant x \leqslant 0.5$) on the structural, electrical and magnetic properties have been found to be remarkable. Substitution of part of La^{3+} by Sr^{2+} in $LaCoO_3$ converts an equivalent amount of Co^{3+} to Co^{4+} to preserve charge neutrality. Effective magnetic moments (μ_{eff}) obtained from the paramagnetic susceptibility data of all compositions for $x>0$ agree with the calculated spin-only moments assuming that cobalt ions are present as high-spin Co^{3+} and low-spin Co^{IV}.[3,19] But, it has been proposed from electron spectroscopic studies[20] that the cobalt ions exist as low-spin Co^{III} and high-spin Co^{4+}. However, very recent XPS studies suggested that the intermediate spin state is realized in the ferromagnetic phase.[21]

Substitution of La^{3+} by Sr^{2+} in this system gives rise to I–M transition and ferromagnetic ordering for $x>0.18$. Ferromagnetic ordering temperature increases with x and maximum T_c ($\approx$250 K) is observed for $x=0.5$.[2] Recent results from the investigation of the structural[22] and low field magnetic properties[23] in the $La_{1-x}Sr_xCoO_3$ system are of much interest. In the limit $0 \leqslant x \leqslant 0.5$ the crystal structure is rhombohedral but at $x \approx 0.25$ the Co—O distance and Co—O—Co angle in this system showed an abrupt decrease and increase, respectively, and the conductivity behavior changed from semiconducting to metallic. Itoh *et al.*[23] have shown that there is no true long range ferromagnetic order in compounds with $x \geqslant 0.18$. For $x \leqslant 0.18$, the compounds show spin glass behavior due to the frustration of random competing exchange interactions, and in the region $0.18 \leqslant x \leqslant 0.5$ the compounds behave like a cluster glass. An investigation on the static and dynamic response of the cluster glass system $La_{0.5}Sr_{0.5}CoO_3$ was reported recently.[24]

Detailed electron spectroscopic studies[20] on the I–M transition in the $La_{1-x}Sr_xCoO_3$ system gave no indication of a clear emergence of Fermi cut-off in the metallic samples ($x \geqslant 0.2$) as distinct from the insulating ones. However, recent XPS results[25] on $La_{0.5}Ca_{0.5}CoO_3$ showed the features of a Fermi level crossing when compared to that of $LaCoO_3$. Various types of measurements using different techniques on $La_{1-x}Sr_xCoO_3$ were performed on samples processed under different heat treatment conditions and various types of anomalies in the electrical and magnetic properties are reported from time to time. Electron spectroscopic studies[20] were performed on samples processed at 950 °C whereas the work of Itoh *et al.*[23] on the magnetic behavior of various compositions is based on the samples processed at 1300 °C. Various other reports also show that the compounds are processed in the temperature range 950–1300 °C.[2,11,21–27] It thus appears that the reported anomalies in the magnetic, electrical transport and spectroscopic properties may be due to the variation in the processing conditions.

In order to understand the origin of the conflicting results obtained from various studies reported earlier, we have studied the properties of the composition $La_{0.5}Sr_{0.5}CoO_3$ annealed in air at different temperatures, using powder X-ray diffraction, ac magnetic susceptibility, dc magnetization, and resistivity measurements.

Experimental

Polycrystalline $La_{0.5}Sr_{0.5}CoO_3$ samples were prepared by the ceramic method. La_2O_3 (preheated at 1000 °C), $SrCO_3$ and

$CoC_2O_4{\cdot}2H_2O$ were taken in the required stoichiometric ratio and thoroughly mixed in an agate mortar. The mixture was initially heated at 950 °C for 48 h with two intermediate grindings and subsequently at 1000 °C for 72 h in air with six intermediate grindings. 500 mg portions of the ground powder were pressed into the form of a pellet and were annealed in air along with another 500 mg of the powder sample at different temperatures ($1000 \leqslant T_A/°C \leqslant 1300$) for 24 h each with one intermediate grinding (the samples are denoted as given in Table 1). The samples were cooled to room temperature at 100 °C h^{-1}. $La_{0.8}Sr_{0.2}CoO_3$ samples used in this study were also prepared and processed under identical conditions.

All the samples were characterized by powder X-ray diffraction (XRD) using a Philips 1730 X-ray diffractometer (Cu-Kα radiation with Ni filter). Chemical homogeneity was checked by energy dispersive analysis by X-rays (EDAX) using a KEVEX analyzer attached to a JEOL JSM 5200 scanning electron microscope. Oxygen stoichiometry of the samples at room temperature was determined by oxidation–reduction titration using potassium permanganate and iron(II) ammonium sulfate solutions.

Electrical resistivity (dc) measurements[28] in the temperature range $12 \leqslant T/K \leqslant 300$ were made on the sintered pellets (polished and unpolished surfaces) by the four probe van der Pauw method.[29] The ac magnetic susceptibility (ACS) measurements were performed using the mutual inductance technique in an APD cryogenics closed-cycle helium cryostat in the temperature range $15 \leqslant T/K \leqslant 300$ at a frequency of 27 Hz and an applied magnetic field of 10 Oe. The dc magnetization ($H_A = 5000$ Oe) as a function of temperature ($80 \leqslant T/K \leqslant 300$) as well as the field cooled (FC) and zero field cooled (ZFC) measurements ($H_A = 100$ Oe) were done on an EG&G PAR vibrating sample magnetometer (VSM) Model 4500. The saturation magnetization at 80 K was measured at a field of 15 kOe.

Results

Powder XRD patterns of $La_{0.5}Sr_{0.5}CoO_3$ samples annealed at different temperatures are shown in Fig. 1. The patterns are almost identical but those of the low- and high-temperature-annealed samples show asymmetry for some of the reflections. The expanded XRD patterns (in the 2θ range 39.5–42°) of some of the samples are shown in Fig. 2. The XRD peak in this 2θ region corresponds to the (111) reflection from the pseudo-cubic lattice.[26] For LSC1000, a higher angle shoulder is observed in the (111) reflection and this shoulder almost vanished for LSC1200 and reappears for LSC1300. The estimated oxygen stoichiometry of different samples of $La_{0.5}Sr_{0.5}CoO_3$ is given in Table 1. Chemical homogeneity measurements indicated an overall La/Sr ratio ≈1 for all the samples, within the error of EDAX measurements. When measured on individual grains, the ratio was found to vary from grain to grain for the low-temperature annealed samples. For LSC1200 this ratio ≈1 with no appreciable variation from grain to grain. Oxygen stoichiometry as well as the La/Sr ratio of the $La_{0.8}Sr_{0.2}CoO_3$ samples also showed similar variations. The value of δ in $La_{0.8}Sr_{0.2}CoO_{3-\delta}$ varied from 0.06 for the sample annealed at 1000 °C to 0.02 for the sample annealed at 1200 °C as observed for $La_{0.5}Sr_{0.5}CoO_3$ (see Table 1).

The normalized resistivity *vs.* temperature curves of the $La_{0.5}Sr_{0.5}CoO_3$ samples (measured on polished pellets) annealed at different temperatures are shown in Fig. 3. The resistivity curves show the metallic nature of the samples exhibiting a slope change at *ca.* 250 K, which is close to the Curie temperature, T_c, for this composition.[30] At all temperatures, the resistivity values are higher for the samples annealed below 1150 °C and maximum variation in the resistivity is obtained for LSC1150. For $T_A > 1150$ °C, a broad maximum

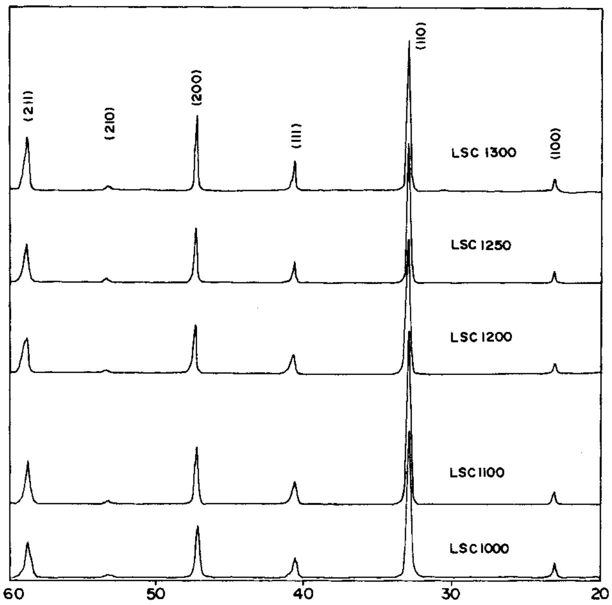

Fig. 1 Powder X-ray diffraction patterns of $La_{0.5}Sr_{0.5}CoO_3$ annealed at various temperatures in the range 1000–1300 °C. The patterns are indexed on a pseudo-cubic lattice. The labels on the curves indicate sample codes as defined in Table 1.

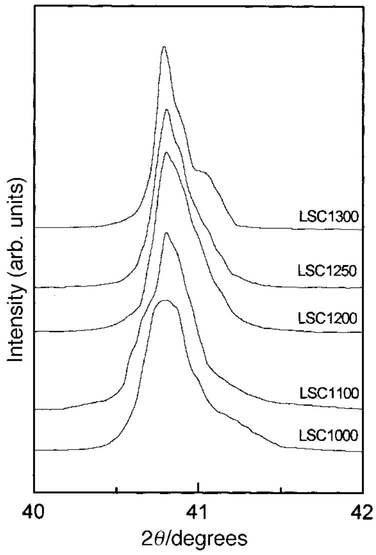

Fig. 2 Powder XRD pattern showing the (111) reflection from the pseudo-cubic lattice of $La_{0.5}Sr_{0.5}CoO_3$ annealed at different temperatures. The labels on the curves indicate sample codes as defined in Table 1.

Table 1 Details of $La_{0.5}Sr_{0.5}CoO_3$ annealed at various temperatures, along with the room temperature resistivity, and the magnetic ordering temperatures obtained from the ac susceptibility measurements

Sample code	Annealing temperature/°C; duration/h[a]	Oxygen content (±0.02)	ρ(300 K)/ mΩ cm	T_c/K	$T_{\chi max}$/K
LSC1000	1000; 72	2.95	0.75	251	232
LSC1100	1100; 24	2.96	0.62	250	226
LSC1101	1100; 48	2.98	—	250	230
LSC1130	1130; 24	2.98	—	249	230,248
LSC1150	1150; 24	2.99	0.30	252	247
LSC1200	1200; 24	2.98	0.28	250	247
LSC1250	1250; 24	2.98	0.25	248	246
LSC1300	1300; 24	2.95	0.22	246	238

[a]Compound was initially heated at 950 °C; 48 h.

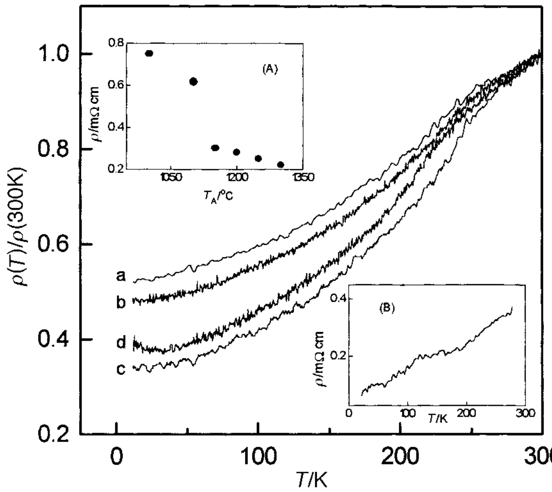

Fig. 3 $\rho(T)/\rho(300\ K)$ curves of the $La_{0.5}Sr_{0.5}CoO_3$ samples annealed at different temperatures; (a) 1000 °C, (b) 1100 °C, (c) 1150 °C, (d) 1300 °C. Insets: (A) Room temperature resistivity, $\rho(300\ K)$, as a function of annealing temperature, T_A; (B) $\rho(T)$ curve of the sample annealed at 1200 °C, measured on the unpolished surface of the pellet.

centered around 150 K is observed apart from the T_c anomaly, for the unpolished pellets. This is shown for LSC1200 in the inset B of Fig. 3 (LSC1250 and LSC1300 also showed identical behavior). This behavior is not observed in the resistivity data of those samples annealed at or below 1150 °C. The feature at 150 K was not observed when measurements were made after polishing the surface of the pellets. As T_A is increased, the room temperature resistivity value is decreased. An abrupt change in room temperature resistivity is observed for the sample annealed above 1100 °C as shown in the inset A of Fig. 3.

The temperature variations of ac susceptibility (ACS) of the $La_{0.5}Sr_{0.5}CoO_3$ samples annealed at different temperatures are shown in Fig. 4. Values of T_c obtained from the temperature derivative of susceptibility and $T_{\chi max}$ are given in Table 1. It may be noted that the T_c is almost a constant, *ca.* 250 K, for the samples annealed up to 1150 °C and decreases continuously for the samples annealed above this temperature. There is no significant change in the maximum value of the susceptibility or the position of the broad maximum after annealing the sample at 1100 °C for longer duration (inset of Fig. 4).

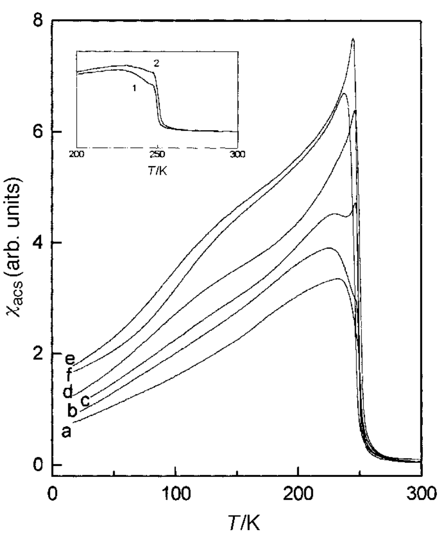

Fig. 4 Temperature variation of the ac susceptibility of $La_{0.5}Sr_{0.5}CoO_3$ samples annealed at different temperatures; (a) 1000 °C, (b) 1100 °C, (c) 1130 °C, (d) 1150 °C, (e) 1250 °C and (f) 1300 °C. Inset: ACS curves of the sample annealed at 1100 °C for (1) 24 h and (2) 48 h.

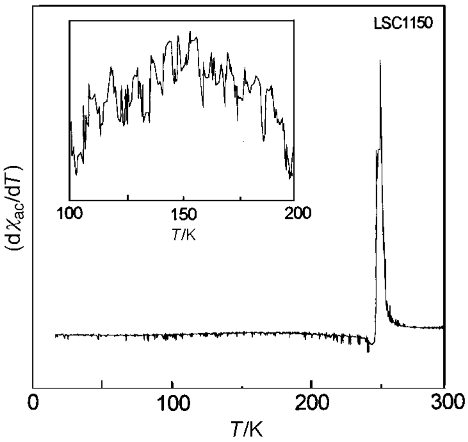

Fig. 5 Temperature variation of the derivative of the ac susceptibility ($d\chi_{ac}/dT$) of $La_{0.5}Sr_{0.5}CoO_3$ sample annealed at 1150 °C. Inset shows the expanded curve in the temperature range 100–200 K.

The sample annealed at 1130 °C shows the features of the ACS curves of both LSC1100 and LSC1150. A broad feature with a shoulder-like behavior appeared below 180 K in the ACS curve of LSC1150, which is not visible in the susceptibility curves of the low-temperature-annealed samples. The peak at $T_{\chi max}$ is slightly broadened for LSC1300 compared to LSC1250 and the magnitude of the low-temperature feature also is enhanced compared to that of other samples.

Fig. 5 shows the derivative of the ac susceptibility, $d\chi_{ac}/dT$, of LSC1150 plotted *vs.* temperature. The sharp peak at 252 K is at the T_c. The inset of Fig. 5 shows the derivative in the temperature range 100–200 K. A broad maximum centered around 150 K is clearly visible in the figure.

The magnetization *vs.* temperature curves of the samples annealed at various temperatures are shown in Fig. 6. It appears that for the low-temperature-annealed samples, T_c is lower than that of the high-temperature-annealed samples and T_c continuously increased as T_A is increased. The inset of Fig. 6 shows the normalized magnetization curves which clearly shows the sharp magnetic transition of the high temperature annealed sample. The magnetization measured at 80 K at a field strength of 15 kOe is *ca.* 25 emu g^{-1} for LSC1000 and *ca.* 40 emu g^{-1} for LSC1250. Fig. 7 shows the magnetization curves of $La_{0.8}Sr_{0.2}CoO_3$. T_c is decreased from *ca.* 250 K to *ca.* 180 K as T_A is increased from 1000 to 1200 °C. This behavior is opposite to that observed for $La_{0.5}Sr_{0.5}CoO_3$.

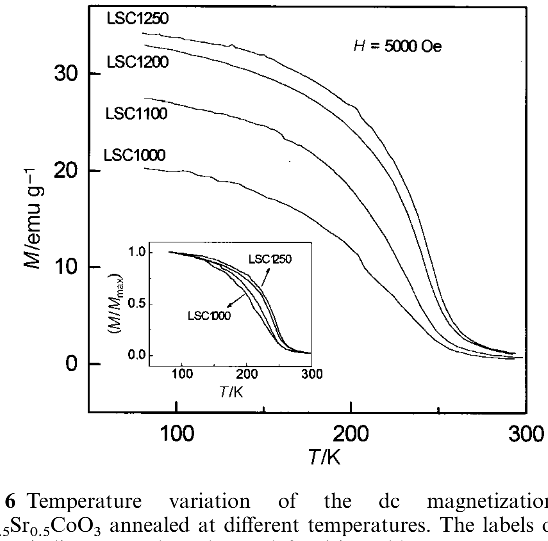

Fig. 6 Temperature variation of the dc magnetization of $La_{0.5}Sr_{0.5}CoO_3$ annealed at different temperatures. The labels on the curves indicate sample codes as defined in Table 1. Inset: normalised magnetization (M/M_{max} *vs.* T) curves showing the increasing sharpness of the magnetic transition as the annealing temperature is increased.

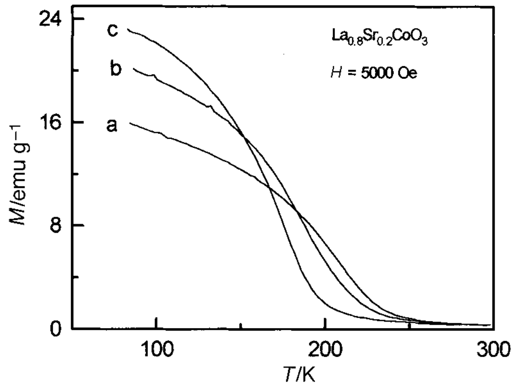

Fig. 7 Temperature variation of the dc magnetization of $La_{0.8}Sr_{0.2}CoO_3$ annealed at different temperatures; (a) 1000 °C, (b) 1100 °C, (c) 1200 °C.

The FC and ZFC magnetization curves of the samples LSC1000, LSC1200 and LSC1300, measured at an applied field (H_A) of 100 Oe, are shown in Fig. 8. A sharp magnetic transition at *ca.* 250 K is observed for LSC1200 and LSC1300 whereas the magnetic transition is very broad for LSC1000. For LSC1200 and LSC1300 a change in slope for the ZFC curve is observed below 160 K. Fig. 9 shows the temperature derivative of the ZFC (dM_{ZFC}/dT) curves of LSC1000 and LSC1200. A sharp peak at the Curie temperature is obtained for LSC1200 whereas multiple broad peaks are seen for LSC1000.

Discussion

Structure

The powder XRD patterns recorded in a wide 2θ range ($10 \leqslant 2\theta/° \leqslant 80$) did not show any extra reflections which indicate the absence of unreacted starting compounds or impurity phases. The absence of any extra reflections in the powder XRD pattern of the samples processed at different temperatures has been attributed in the literature[11,20,23,26] to the 'single-phase' behavior of $La_{0.5}Sr_{0.5}CoO_3$. However, the present detailed X-ray diffraction analysis revealed a minor structural dissimilarity between the low- and high-temperature-

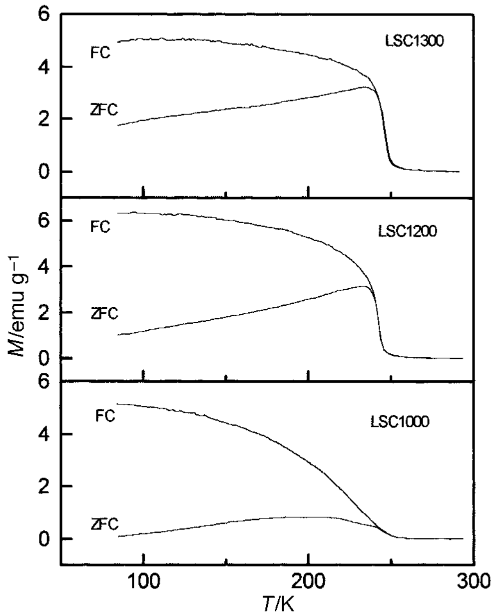

Fig. 8 Temperature variation of the field cooled (FC) and the zero field cooled (ZFC) curves of LSC1000, LSC1200 and LSC1300 at a field of 100 Oe. The labels indicate sample codes as defined in Table 1.

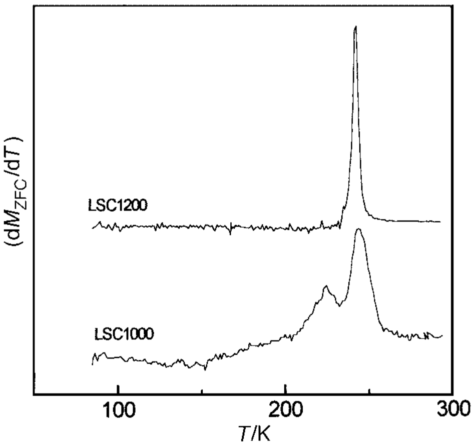

Fig. 9 Temperature variation of the derivative of M_{ZFC} (dM_{ZFC}/dT) of LSC1000 and LSC1200. The labels indicate sample codes as defined in Table 1.

annealed samples (Fig. 2). For the $La_{1-x}Sr_xCoO_3$ system, the rhombohedral angle, α, varies linearly from 60.05 to 60.8° between $x=0.5$ and $x=0.0$ (ref. 22). For the rhombohedral lattice, the pseudo-cubic (111) reflection corresponds to (202) and (006) reflections and the difference in the position between the two reflections for $La_{0.5}Sr_{0.5}CoO_3$ is less than 0.2° so that they appear as a single peak in the XRD pattern as observed for LSC1200. Therefore the high angle shoulder in the XRD peak (Fig. 2) of the samples annealed below 1150 °C and above 1250 °C can only be accounted if it is assumed that extra phase(s) with slightly differing composition(s) (or oxygen deficiency) are present in the sample apart from the $x=0.5$ composition. The possibility of line broadening due to lower particle size of low-temperature-annealed samples can be ruled out as the XRD pattern is asymmetric rather than broad. Also, the particle size of the samples annealed in the temperature range 1000–1300 °C (obtained from SEM) varied only from 0.5–1 μm and hence the line broadening due to these particles will be much less than the observed splitting/asymmetry. Thus the asymmetry of the XRD peak of the low-temperature-annealed samples is due to compositional inhomogeneity because of the presence of La-rich phases which are rhombohedral. The small rhombohedral splitting may not be visible in the powder XRD patterns recorded in a wide 2θ range due to the compressed scale and hence the powder XRD patterns recorded in a wide 2θ range appear to be identical for all the samples. Battle *et al.*[31] have recently addressed the inability of powder XRD patterns to show the presence of different compositions of a solid solution in a sample of the layered manganates and used a two phase model in the Rietveld refinement of the X-ray diffraction pattern. It has been shown that separation into different phases is apparent only on detailed inspection of the profile.

Oxygen stoichiometry

Oxygen stoichiometry measurements are usually carried out as part of the characterization of the cobaltates.[2,20,22,26] It is known that at high values of x in $La_{1-x}Sr_xCoO_3$ an oxygen non-stoichiometry effect is predominant.[2,19] Oxygen stoichiometry measurements at room temperature indicate (see Table 1) that near-stoichiometric composition is obtained for samples annealed between 1150 and 1250 °C. The large deviation from full oxygen stoichiometry for the low-temperature-annealed samples is an evidence for compositional inhomogeneity because it is unlikely that the low-temperature-annealed samples are oxygen deficient. Jonker and Van Santen[2] have reported that firing at very high temperatures causes appreciable loss of oxygen from the sample. If various phases with locally differing La and Sr compositions, whose macroscopic average give $La_{0.5}Sr_{0.5}CoO_3$, are present in the samples, then the calculated oxygen content will be different from what is expected. This is because the Sr-rich compositions will be highly oxygen deficient when annealed in air.[19] Since a homogeneous phase is obtained for $T_A \geq 1150\,°C$, the lower oxygen content of LSC1300 may be understood in terms of oxygen loss from the sample because the oxygen loss from the sample is very high at higher processing temperatures.[2,32] So the sample heated at higher temperatures when cooled back to room temperature will be oxygen deficient compared to the sample heated to a lower temperature. The reappearance of the rhombohedral splitting in the XRD pattern (Fig. 2) may be attributed to this oxygen deficiency. Thus, it appears that the compound annealed below 1150 °C is compositionally inhomogeneous and that annealed above 1250 °C is compositionally non-stoichiometric (oxygen deficient).

Composition

Further evidence for compositional inhomogeneity for the sample annealed below 1150 °C is obtained from EDAX analysis. It has been pointed out earlier[33] from EDAX analysis that compositional inhomogeneity exists in compounds such as $(LaSr)MnO_3$ and $(LaSr)CrO_3$ when processed at low temperatures and even in the sample heated to 1400 °C. When the compositions of individual particles were measured, it was found that the composition varied from particle to particle and all compositions in the entire range $0 \leqslant x \leqslant 1$ were observed in the low-temperature-processed samples of a nominal composition $La_{0.5}Sr_{0.5}MnO_3$. Similarly, in the present case, the difference in the La/Sr ratio on different grains of LSC1000 shows microscopic non-homogeneity arising due to the presence of Sr-rich (La-deficient) and Sr-deficient (La-rich) regions within the sample. The La/Sr ratio of LSC1200 is close to unity and is uniform throughout the sample suggesting a uniform distribution of La^{3+}/Sr^{2+} and the formation of a compositionally homogeneous $La_{0.5}Sr_{0.5}CoO_3$. The local variation of the La/Sr ratio as well as oxygen deficiency affects the distribution of Co^{3+} and Co^{4+} in the lattice. This will directly affect the electrical and magnetic properties of $La_{0.5}Sr_{0.5}CoO_3$.

Electrical properties

Differences in the behavior of the resistivity curves of different samples (Fig. 3) can be explained in terms of the distribution of Co^{3+}/Co^{4+} in these samples. Although the low-temperature-annealed samples are non-homogeneous, they still show metallic behavior. The T_c anomaly[30] is observed for all the curves but maximum drop in resistivity below the T_c is observed for the sample annealed at 1150 °C (nearly 33% drop in resistivity in the range 200–250 K for LSC1150 whereas <18% drop for LSC1000 and LSC1100 in the same temperature range). When the compound is compositionally homogeneous, the Co^{3+}/Co^{4+} ratio = 1 throughout the sample and a sharp T_c anomaly can be expected. Deviation of this ratio from unity shifts the T_c to lower temperatures.[19] Hence a well defined T_c anomaly may not be seen for an inhomogeneous sample. The continuous decrease of the room temperature resistivity with the increase in annealing temperature is due to the improved homogeneity as well as due to the increased compactness of the pellets at higher annealing temperatures. The large difference between the room temperature resistivity values of the sample annealed at 1100 and 1150 °C (Table 1 and inset A of Fig. 3) and maximum variation of the resistivity with temperature for the sample annealed at 1150 °C compared to that of the samples annealed above and below this temperature indicates a uniform Co^{3+}/Co^{4+} distribution in the sample processed at 1150 °C. The upturn at 30 K in the resistivity curve of LSC1300 (Fig. 3) may be explained in terms of oxygen deficiency (Table 1). Recently, Chan *et al.*[34] and Madhukar *et al.*[35] have reported the resistivity behavior of thin-film samples of $La_{0.5}Sr_{0.5}CoO_3$ processed at different temperatures and conditions. They have shown that the stoichiometric $La_{0.5}Sr_{0.5}CoO_3$ films are metallic as against a semiconducting transport behavior for oxygen deficient films. The slightly higher resistivity values at low temperatures for LSC1200 and LSC1250 compared to that of LSC1150 also can be accounted to the presence of an oxygen deficient insulating phase in the high-temperature-annealed samples. The anomaly (broad feature) at 150 K in the resistivity curve (inset B of Fig. 3) disappeared after removing the surface layer from the sample pellet. Examination of the surface as well as the interior part of a LSC1200 pellet by XRD and EDAX analysis did not show any evidence for the presence of extra phases or variation in the La/Sr ratio. This shows that probably a very thin layer, of thickness much less than the electron penetration depth, is formed as a secondary phase on the surface.

ac susceptibility

The contribution from the $x=0.5$ phase in the ACS curve (Fig. 4) is <50% for LSC1000 as evidenced from the magnitude of the susceptibility at $T_{\chi max}$ compared to that of LSC1250. χ_{max} increases with annealing temperature and there is no considerable change in the T_c of samples annealed up to 1150 °C (Table 1). This implies that the amount of $La_{0.5}Sr_{0.5}CoO_3$ is increased as the annealing temperature is increased and this phase is stoichiometric, though the entire sample is compositionally inhomogeneous (in other words, the compositional range narrowed down as the annealing temperature is increased, as reported in ref. 33). Some other important observations from the ACS results are; (i) the difference between T_c and $T_{\chi max}$ (*i.e.* $T_c - T_{\chi max}$) is minimum for the high temperature sharp peak of the sample annealed at 1130 °C, and (ii) T_c is maximum for the 1150 °C annealed sample. It may be expected that $T_c - T_{\chi max}$ will be minimum for a single phase composition as observed for the stoichiometric compound $SrRuO_3$,[36,37] where $T_c - T_{\chi max} = 1$ K. The ACS behavior of LSC1150 is found to be almost identical to that of $SrRuO_3$. Observation of a large difference in the $T_c - T_{\chi max}$ value or more than one peak in the ac susceptibility curve (as observed for LSC1130) thus shows the presence of extra phases with different compositions. The shift of T_c and $T_{\chi max}$ to lower temperatures for LSC1300 can be explained in terms of oxygen deficiency. The increase in oxygen deficiency increases the Co^{3+} content compared to Co^{4+}. Since the exchange interaction $Co^{3+}{-}O{-}Co^{4+}$ is known to be ferromagnetic and the $Co^{3+}{-}O{-}Co^{3+}$ interaction is antiferromagnetic, a decrease in the T_c is expected. The fact that $T_c - T_{\chi max}$ is minimum (1 K) for the high temperature sharp peak in the ACS curve of LSC1130, the T_c is maximum for LSC1150, and the extra feature at 150 K in the ACS curves starts appearing after annealing at 1150 °C and above, suggest the difficulty to stabilize a pure and compositionally homogeneous phase of $La_{0.5}Sr_{0.5}CoO_3$. A true ferromagnetic composition, thus, may form in a narrow temperature region between 1130 and 1150 °C. However, it is possible that the temperature range which gives a single phase compound may vary depending on the atmosphere in which the sample is annealed.

The broad feature in the derivative ac susceptibility curve (inset of Fig. 5) as well as in the resistivity curve of LSC1200 (inset B of Fig. 3) is almost in the same temperature region and can be attributed to the contribution from an oxygen deficient phase since it appears only in high-temperature-annealed samples. It may be assumed that oxygen deficiency at the surface of a particle/pellet of the compound is higher than that in the bulk. The broad feature around 150 K was also observed in the field dependent dc magnetization studies[24] of $La_{0.5}Sr_{0.5}CoO_3$. This feature showed frequency as well as magnetic field dependence. Itoh *et al.*[23] have found that for $x=0.18$ the magnetic transition temperature is close to 150 K and shows the characteristic features of a spin glass[38] system. As the additional feature in the ac susceptibility curve is centered around 150 K, the Co^{3+}/Co^{4+} ratio on the surface will be close to that of $x\approx0.18$ in $La_{1-x}Sr_xCoO_3$. However, one has to look into this 150 K feature also in terms of the Hopkinson effect,[39] which is the observation of a secondary peak (at a certain temperature below the main peak at the Curie temperature) in the permeability *vs.* temperature curve of a ferromagnetic system.[40,41] The secondary maximum is observed when measured only at very small magnetic fields and vanishes at higher measuring fields.

dc magnetization

For LSC1000 the dc magnetization curve (Fig. 6) is very broad and appears as if the T_c of this sample is lower than that of the actual T_c of $La_{0.5}Sr_{0.5}CoO_3$. However, the T_c values obtained from the ACS curves are comparable for all the samples. Thus, the apparent low T_c of LSC1000 is due to the coexistence of different compositions of $La_{1-x}Sr_xCoO_3$ with varying x values whose magnetic ordering temperatures are different.[42] The sum of the magnetization curves of these individual phases when plotted against temperature will appear as a broad magnetic transition.

Since maximum T_c in the $La_{1-x}Sr_xCoO_3$ series is for the $x=0.5$ composition, the presence of the low-T_c phases is not directly evident in the magnetization curves shown in Fig. 6. $La_{0.8}Sr_{0.2}CoO_3$, whose T_c is lower than the maximum T_c of $x=0.5$, shows direct evidence for compositional inhomogeneity in its magnetization curves (Fig. 7). This compound is expected to show a ferromagnetic transition at *ca.* 180 K.[10,23] However, for the sample annealed at 1000 °C there is an increase in the magnetization at *ca.* 250 K. A marked increase in the susceptibility at *ca.* 240 K for the compositions with $0\leqslant x\leqslant0.15$ in $La_{1-x}Sr_xCoO_3$ was earlier assigned to the onset of magnetic order within superparamagnetic clusters, for samples synthesized by the coprecipitation method and annealed at 1000 °C.[26] Similarly for compositions with $0.2\leqslant x\leqslant0.5$ also the transition temperature varied only between $T_c\approx250$ K at $x=0.2$ and $T_c\approx255$ K at $x=0.5$. The independence of T_c with x has been attributed to the disproportionation of the compounds into two phases. Ac susceptibility measurements on the spin glass composition $La_{0.85}Sr_{0.15}CoO_3$ synthesized by the ceramic method and annealed at 1000 °C showed a sharp magnetic transition at *ca.* 250 K, the shape of the curve was similar to that of $La_{0.5}Sr_{0.5}CoO_3$.[43] A clear cusp in the ac susceptibility curve at the spin glass freezing temperature, as reported by Itoh *et al.*,[23] was observed only after annealing the sample at 1300 °C for a long duration, Therefore, for the $La_{0.8}Sr_{0.2}CoO_3$ sample also, the increase in the magnetization at *ca.* 250 K implies the presence of the $x=0.5$ phase (Sr-rich phase) when annealed at low temperatures. At higher annealing temperatures the contribution due to the Sr-rich phases decreases and T_c shifts to lower temperatures, as observed for $La_{0.85}Sr_{0.15}CoO_3$. Finally a compositionally homogeneous phase is obtained with $T_c\approx180$ K after annealing at 1200 °C. Thus, these results are consistent with the conclusion drawn from the EDAX and powder XRD analyses that low temperature processed samples are compositionally inhomogeneous.

The FC and ZFC results (Fig. 8) of $La_{0.5}Sr_{0.5}CoO_3$ show the absence of true long range ferromagnetic ordering,[23] since a large thermoremanent magnetization at 80 K is observed for LSC1000, LSC1200 and LSC1300 samples. The sharp rise in the FC and ZFC magnetizations at 250 K for LSC1200 and LSC1300 is an evidence for a finite-range ferromagnetic ordering. It may be assumed that lack of true long-range FM ordering is due to the formation of finite-size ferromagnetic clusters which orders at a quasi-critical temperature. The presence of excess Co^{3+} in the sample hinders the true long-range Co^{3+}—O—Co^{4+} exchange interaction which in turn decides the size of the ferromagnetic clusters. Hence we believe that the magnitude of $T_c-T_{\chi max}$ in the ac susceptibility curve will have a strong dependence on the size of the ferromagnetic clusters. The comparatively low value of the ZFC magnetization of LSC1000 at 250 K as against that of LSC1200 and LSC1300 supports the conclusion drawn from the ACS studies that less than 50% of the sample contains the true $La_{0.5}Sr_{0.5}CoO_3$ phase.

The continuous increase of the FC magnetization of LSC1000 down to 80 K indicates the contribution from a paramagnetic phase superimposed on that from a ferromagnetic phase. The paramagnetic phase arises from the presence of compositions with $x<0.5$ whose T_c continuously shifts to lower temperatures as x is decreased to zero. The low temperature ^{57}Co Mössbauer spectroscopic studies[44] on the $La_{1-x}Sr_xCoO_3$ compounds also revealed the presence of a paramagnetic phase (PM) in the ferromagnetic (FM) compositions. The true magnetic behavior of these compounds was explained on the basis of the occurrence of ferromagnetic clusters of varying sizes in a paramagnetic matrix. The present study suggests that the paramagnetic phase is due to the presence of La-rich phases in this composition. The broad maximum at *ca.* 200 K in the M_{ZFC} curve and the broad magnetic transition in the M_{FC} curve of LSC1000 sample are due to superimposition of a large number of curves (for different x values) of the type obtained for LSC1200. This aspect can be distinctly seen in the dM_{ZFC}/dT *vs.* T curves given in Fig. 9. The derivative curve of LSC1200 gives a sharp peak at the Curie temperature whereas for LSC1000 multiple broad peaks are seen. The most intense peak in the derivative curve for LSC1000 is at the T_c of $La_{0.5}Sr_{0.5}CoO_3$ and the second most intense peak is at *ca.* 230 K where ACS measurement gave a broad peak. The change in slope of the ZFC curves of LSC1200 and LSC1300 below 160 K (since ZFC measurements were performed at a sufficiently higher field of 100 Oe, this feature is not seen as distinctly as in the ACS curves which were measured at 10 Oe) supports the conclusions drawn from the resistivity and the ACS studies. The M_{ZFC} curve shown by Itoh *et al.*[23] for the composition $La_{0.5}Sr_{0.5}CoO_3$ shows a slope change near 150 K for the sample annealed at 1300 °C and the overall nature of the curve is similar to that of LSC1300.

Most of the anomalies and discrepancies reported in the literature on the electronic and magnetic properties of the $La_{1-x}Sr_xCoO_3$ system can, now, be explained in the light of the present study. The absence of a clear emergence of the Fermi cut-off in the metallic samples as distinct from the insulating samples of $La_{1-x}Sr_xCoO_3$ observed from electron spectroscopic studies[20] can be explained in terms of compositional inhomogeneity of the samples processed at 950 °C. Because of this compositional inhomogeneity, a close control over the true composition is not possible for samples processed at low temperatures, which prevents a clear transition from the insulating phase to the metallic phase on Sr doping. The low Fermi level density of states of the metallic phase is due to the presence of a lanthanum-rich insulating phase which increases the room temperature resistivity. On the other hand, Saitoh *et al.*[21] have reported that the valence band spectra show systematic changes and reflect the semiconductor–metal transition with Sr doping, for those samples processed at 1300 °C with subsequent oxygen treatment.

A metallic behavior with a well defined T_c anomaly is reported for polycrystalline[10] as well as single-crystal[8] $La_{0.8}Sr_{0.2}CoO_3$. The insulating behaviour of the same composition is also reported.[11,26] As $La_{0.8}Sr_{0.2}CoO_3$ falls near the I–M transition region, a local deviation of the Co^{3+}/Co^{4+} ratio can drastically affect the resistivity behavior of this composition. Hence the insulating nature obtained[11,26] for the compound may be attributed to the low processing temperature resulting in compositional inhomogeneity as against the high temperature processed metallic samples. The upturn in the resistivity curves[11,26] at low temperature for the metallic samples and the presence of a magnetic transition at *ca.* 240 K reported for $x<0.5$ compositions[26,45] also can be explained within this framework.

Conclusions

Electrical resistivity, low field ac magnetic susceptibility and dc magnetization at low (FC and ZFC) and high magnetic fields are measured as a function of temperature to study the effect of processing conditions on these properties of the system $La_{0.5}Sr_{0.5}CoO_3$. These measurements indicate that only the samples annealed at or above 1150 °C showed a compositionally homogeneous $La_{0.5}Sr_{0.5}CoO_3$ with a near-uniform distribution of Co^{3+} and Co^{4+} which determines its metallic and magnetic properties. It is not possible to predict microscopic homogeneity of the compound from powder XRD measurements alone. Oxygen stoichiometry measurements also is not a reliable technique to check the local Co^{3+}/Co^{4+} ratio as it measures only the average oxygen content if various phases are present in the sample. ACS measurement gives information on the extent of chemical homogeneity, as the various phases with different compositions in $La_{1-x}Sr_xCoO_3$ are magnetic with varying magnetic ordering temperatures. The present results suggest that in the low temperature annealed samples, $La_{0.5}Sr_{0.5}CoO_3$ phase co-exists with other phases having different La/Sr ratio. The inconsistencies in the results of various studies reported earlier on $La_{0.5}Sr_{0.5}CoO_3$ could be explained on the basis of the results obtained from the present work.

P.S.A.K. is grateful to University Grants Commission, India, for financial support and to Prof. D. S. Joag for his constant encouragement. We thank Dr (Ms). A. Mitra for XRD and Dr (Ms). A. A. Belhekar for EDAX measurements.

References

1 G. H. Jonker and J. H. Van Santen, *Physica*, 1950, **16**, 337.
2 G. H. Jonker and J. H. Van Santen, *Physica*, 1953, **19**, 120.
3 J. B. Goodenough, *J. Phys. Chem. Solids*, 1958, **6**, 287.
4 J. B. Goodenough and J. M. Longo, *Landolt-Bornstein New Series Group III*, Springer-Verlag, Berlin, 1970, vol. IVa, p. 126.
5 C. W. Searle and S. T. Wang, *Can. J. Phys*., 1970, **48**, 2024.
6 J. B. Goodenough, *Prog. Solid State Chem*., 1971, **5**, 145.
7 A. P. Ramirez, *J. Phys.: Condens. Matter*, 1997, **9**, 8171.
8 S. Yamaguchi, H. Taniguchi, H. Takagi, T. Arima and Y. Tokura, *J. Phys. Soc. Jpn*., 1995, **64**, 1885.
9 G. Briceno, H. Chang, X. Sun, P. G. Schultz and X. -D. Xiang, *Science*, 1995, **270**, 273.
10 V. Golovanov, L. Mihaly and A. R. Moodenbaugh, *Phys. Rev. B*, 1996, **53**, 8207.
11 R. Mahendiran and A. K. Raychaudhuri, *Phys. Rev. B*, 1996, **54**, 16 044.
12 P. G. Radaelli, D. E. Cox, M. Mareio, S. W. Cheong, P. E. Schiffer and A. P. Ramirez, *Phys. Rev. Lett*., 1995, **74**, 4488.
13 H. Kuwahara, Y. Tomioka, A. Asamitsu, Y. Moritomo and Y. Tokura, *Science*, 1995, **270**, 961.
14 I. Bozovic, J. H. Kim, J. S. Harris, Jr., C. B. Eom, J. M. Philips and J. T. Cheung, *Phys. Rev. Lett*., 1994, **73**, 1436.
15 P. M. Raccah and J. B. Goodenough, *Phys. Rev*., 1967, **155**, 932.
16 G. Thornton, B. C. Tofield and A. W. Hewat, *J. Solid State Chem*., 1986, **61**, 301.
17 M. Abbate, J. C. Fuggle, A. Fujimori, L. H. Tjeng, C. T. Chen, R. Potze, G. A. Sawatzky, H. Eisaki and S. Uchida, *Phys. Rev. B*, 1993, **47**, 16124.
18 T. Saitoh, T. Mizokawa, A. Fujimori, M. Abbate, Y. Takeda and M. Takano, *Phys. Rev. B*, 1997, **55**, 4257.
19 H. Taguchi, M. Shimada and M. Koizumi, *Mater. Res. Bull*., 1978, **13**, 1225.
20 A. Chinani, M. Mathew and D. D. Sarma, *Phys. Rev. B,* 1992, **46**, 9976.
21 T. Saitoh, T. Mizokawa, A. Fujimori, M. Abbate, Y. Takeda, and M. Takano, *Phys. Rev. B*, 1997, **56**, 1290.
22 A. Mineshige, M. Inaba, T. Yao, Z. Ogumi, K. Kikuchi and M. Kawase*, J. Solid State Chem*., 1996, **121**, 423.
23 M. Itoh, I. Natori, S. Kubota and K. Motoya, *J. Phys. Soc. Jpn*., 1994, **63**, 1486.
24 S. Mukherjee, R. Ranganathan, P. S. Anil Kumar and P. A. Joy, *Phys. Rev. B*, 1996, **54**, 9267.
25 R. P. Vasquez, *Phys. Rev. B*, 1996, **54**, 14938.
26 M. A. Senaris-Rodriguez and J. B. Goodenough, *J. Solid State Chem*., 1995, **118**, 323.
27 K. Asai, O. Yokokura, N. Nishimori, H. Chou, J. M. Tranquada, G. Shirane, S. Higuchi, Y. Okajima and K. Kohn, *Phys. Rev. B*, 1994, **50**, 3025.
28 K. Sreedhar and P. A. Joy, *Solid State Commun*., 1996, **99**, 589.
29 L. J. van der Pauw, *Philips Res. Rep*., 1958, **13**, 1.
30 N. Menyuk, P. M. Raccah and K. Dwight, *Phys. Rev*., 1968, **166**, 510.
31 P. D. Battle, M. A. Green, N. S. Laskey, J. E. Millburn, L. Murphy, M. J. Rosseinsky, S. P. Sullivan and J. F. Vente, *Chem. Mater*., 1997, **9**, 552.
32 A. N. Petrov, V. A. Cherepanov, O. F. Kononchuk and I. Y. Gavrilova, *J. Solid State Chem*., 1990, **87**, 69.
33 M. S. G. Baythoun and F. R. Sale, *J. Mater. Sci*., 1982, **17**, 2757; L. A. Chick, L. R. Pederson, G. D. Moupin, J. L. Bates, L. E. Thomas and G. J. Exarhos*, Mater. Lett*., 1990, **10**, 6.
34 P. W. Chan, W. Wu, K. H. Wong, K. Y. Tong and J. T. Cheung*, J. Phys. D: Appl. Phys*., 1997, **30**, 957.
35 S. Madhukar, S. Aggarwal, A. M. Dhote, S. Ramesh, A. Krishnan, D. Keeble and E. Poindexter, *J. Appl. Phys*., 1997, **81**, 3543.
36 P. A. Joy, S. K. Date and P. S. Anil Kumar, *Phys. Rev. B*., 1997, **56**, 2324.
37 M. Shikano, T. K. Huang, Y. Inaguma, M. Itoh and T. Nakamura, *Solid State Commun*., 1994, **19**, 115.
38 J. A. Mydosh, *Spin Glasses: An Experimental Introduction*, Taylor & Francis, London, 1993.
39 J. Hopkinson, *Proc. R. Soc. London*, 1890, **48**, 1.
40 S. Tamura, *J. Phys. Soc. Jpn*., 1992, **61,** 752.
41 C. Heck, *Magnetic Materials and their Applications*, Butterworths, London, 1974, p. 9.
42 H. Eisaki, T. Ido, K. Magoshi, M. Mochizuki, H. Yamatsu, T. Ito and S. Uchida, *Physica C*, 1991, **185**, 1295.
43 P. S. Anil Kumar, P. A. Joy and S. K. Date, *J. Appl. Phys*., 1998, **83**, 7375.
44 V. G. Bhide, D. S. Rajoria, C. N. R. Rao, G. Rama Rao and V. G. Jadhao, *Phys. Rev. B*, 1974, **12**, 2832; D. K. Chakrabarty, A. Bandyopadhyay, S. B. Patil and S. N. Shringi, *Phys. Status Solidi A*, 1983, **79**, 213.
45 J. Mira, J. Rivas, R. D. Sanchez, M. A. Senaris-Rodriguez, D. Fiorani, D. Rinaldi and R. Caciuffo, *J. Appl. Phys*., 1997, **81**, 5753.

Paper 8/02952K